Line Shape of the Mössbauer Line in the Presence of Ultrasonic Vibrations with Decaying Amplitudes

GERTRUDE KORNFELD*
University of Albuquerque, Albuquerque, New Mexico 87105

(Received 12 July 1968)

A Mössbauer source that executes ultrasonic vibrations with decaying amplitudes has a center-line fraction that increases with time; the center line of the emitted radiation can be even narrower than half the natural width. The nth band fraction has its maximum when $k^2\langle x^2\rangle \approx n^2$; sidebands can be either narrowed or widened; narrowing can take place with large initial amplitudes that decrease or small initial amplitudes that increase. Random fluctuations in ultrasonic amplitudes might explain the narrow side bands in Cranshaw and Reivari's ultrasonic experiment as a superposition of widened and narrowed lines.

1. INTRODUCTION

IT was theoretically established by Nussbaum and Dash[1] that the simultanous decay of the state of excitation of a localized lattice vibration mode and of the Mössbauer nucleus narrows the Mössbauer line beyond its natural width. They showed that such narrowing can take place in an extremely short-lived Mössbauer source that did not reach thermal equilibrium. Harris[2] performed a quantum-mechanical derivation of this nonequilibrium situation and established a line narrowing of 36% under the most favorable conditions.

In this paper, line narrowing caused by ultrasonic vibrations with decaying amplitudes will be analyzed. This narrowing can be regarded as an ultrasonic analog of the cooling source, where the amplitude of a localized lattice vibration mode decays. The important advantages are as follows: (a) The simplicity of the conditions enables the consideration of all higher-order terms. (b) Not only the center line but all sidebands can be analyzed. (c) Line narrowing caused by ultrasonic vibrations with decaying amplitudes might be experimentally verified.

An important distinction is the low frequency of the ultrasonic vibrations, compared to the high frequencies of localized lattice vibration modes in the cooling source. Very many small quanta of ultrasonic energy have to be added coherently; a classical description is as natural to the problem as a coherent quantum-mechanical one. During the average Mössbauer nuclear excited-state lifetime, the ultrasonic mode is lowered by very many quanta. Restrictions on line narrowing established by Harris[2] for the lowering of the localized lattice vibration mode by one quantum do not apply to the ultrasonic analog. Line narrowing of more than 50% with a line depth of the order of 1% is in the realm of possibility.

This percentage of line narrowing applies to the spectral distribution of the radiation leaving the source but not to the observable, which is the radiation transmitted through the absorber. In most Mössbauer studies the distinction is of small importance because usually a thin absorber only increases the linewidth from Γ_S to $\Gamma_S+\Gamma_A$ without changing the line shape. Here the subscripts S and A mean source and absorber, respectively.

In the presence of ultrasonic vibrations with decaying amplitudes the fraction of the radiation belonging to the nth band, $f_n(t)$, is time-dependent; if $f_n(t)$ increases during the average Mössbauer nuclear excited-state lifetime the line is narrowed; if $f_n(t)$ decreases the line is widened. The presence of the absorber does not influence the time dependence of $f_n(t)$ but changes the time interval that has to be analyzed; in cases where the slope of $f_n(t)$ changes sign during the average Mössbauer nuclear excited-state lifetime it is possible that the linewidth at half-height of the radiation leaving the source, $\Gamma_S(\text{eff})>\Gamma_S$, but that the linewidth of the observable, $\Gamma(\text{eff})<\Gamma_S+\Gamma_A$. Tops of such lines are much wider but wings narrower than the Lorentzian shape.

2. REVIEW OF ULTRASONIC MÖSSBAUER STUDIES

In 1960, Ruby and Bolef[3] experimentally established the presence of sidebands at the Doppler-shifted frequencies $\Omega_S-n\omega$ from an ultrasonically vibrating Mössbauer source. Here Ω_S and ω are Mössbauer γ-ray and ultrasonic frequencies, and n can be any positive or negative integer or zero. Their source was thin with respect to the wavelength of the ultrasonic vibrations; therefore, they assumed c.m. motion but only negligible deformation of their source and derived their bands by assuming all Mössbauer nuclei in the source vibrate with the same ultrasonic amplitude, a. Ruby and Bolef's nth-band fractions are

$$f_n\{\text{RB}\} \propto J_n^2(m), \quad m \equiv \mathbf{k}\cdot\mathbf{a}. \tag{1}$$

Here $J_n(m)$ is a Bessel function of the first kind. The wave propagation vector $\mathbf{k}$ was parallel to the amplitude $\mathbf{a}$ in Ruby and Bolef's experiment. The fractions are oscillatory functions of both n and m; for instance, the center-line fractions approach zero when m approaches the values 2.4, 5.5, 8.6, $\cdots$.

* Present address: Night Vision Laboratory, Visionics Technical Area, Fort Belvoir, Virginia 22060.

[1] J. G. Dash and R. H. Nussbaum, Phys. Rev. Letters **16**, 567 (1966).

[2] S. Harris, Phys. Rev. **163**, 280 (1967).

[3] S. L. Ruby and D. I. Bolef, Phys. Rev. Letters **5**, 5 (1960).

Also in 1960, Abragam[4] derived quantum-mechanically the nth band fractions for a source that is not thin with respect to the wavelength of the ultrasonic vibrations; he assumed an abnormally large number compared to equilibrium values of ultrasonic phonons present. Abragam's nth band fractions are

$$f_n\{\mathrm{A}\} \propto e^{-y} I_n(y), \quad y \equiv k^2\langle x^2\rangle. \tag{2}$$

Here $\langle x^2\rangle$ is the projection of the mean-square displacement of the Mössbauer nucleus in the direction of the γ beam, and $I_n(y)=I_{-n}(y)=(-i)^n J_n(iy)$ is a hyperbolic Bessel function.

In 1964, Abragam[5] showed that his Eq. (2) can also be derived classically from Ruby and Bolef's Eq. (1) by assuming a Rayleigh distribution

$$P_1(a)=(a/\langle x^2\rangle)\exp(-\tfrac{1}{2}a^2/\langle x^2\rangle) \tag{3}$$

of amplitudes of ultrasonic vibrations.

In 1967, Cranshaw and Reivari[6] analyzed the sidebands of an ultrasonically vibrating absorber that was not thin. They state that in such an absorber c.m. motion is negligible but that standing and running waves are set up which are reflected back and forth in various directions. Their data, reproduced in Fig. 1, show an excellent fit to Abragam's predicted intensities.

In 1968, Mishory and Bolef[7] derived quantum-mechanically the intensities of the bands for the cases in which the ultrasonic relaxation time is very short and very long. Their rigorous calculations reduce to Abragam's Eq. (2) in the former, and Ruby and Bolef's Eq. (1) in the latter case, after they show that quantum effects are negligible. Experimentally they were able to verify Abragam's equation with the help of an ultrasonically vibrating source that was thick with respect to the thickness of the ultrasonic transducer. Their data is reproduced in Fig. 2.

An important feature of their experiment is the correlation of the line depth of the center line with the ultrasonic driving voltage; they were able to prove excellent linearity. Very interesting is their theoretical explanation and experimental verification of the reduction of the self-absorption of their source in the presence of high-amplitude ultrasonic vibrations.

3. ULTRASONIC VIBRATIONS WITH DECAYING AMPLITUDES

Assume an ultrasonically vibrating source that is not thin with respect to the wavelength of the ultrasonic vibrations and whose Co^{57} nuclei are electroplated on a very thin top layer. It is weak enough that coincidence measurements between the 123-keV photon that announces the formation of the Fe^{57} excited state and the 14.4-keV photon that proves its decay can be performed. If the 123-keV photon is used to remove the driving voltage from the ultrasonic transducer and simultaneously to start the recording of the multichannel analyzer, the effect of ultrasonic vibrations

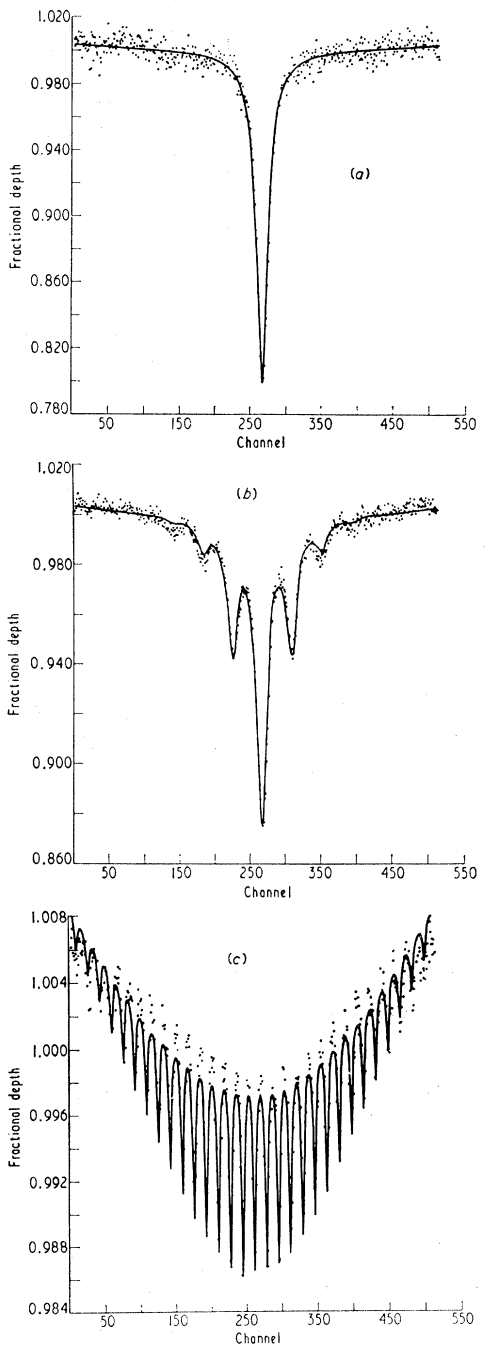

FIG. 1. Cranshaw and Reivari's data. Sideband spectra for an absorber vibrating at the ultrasonic frequency of 16 MHz; the driving voltage across the ultrasonic transducer is (a) $V=0.0$ V, (b) $V=0.4$ V, (c) $V=30.0$ V. In Fig. 1(c) the velocity scale has been contracted by a factor of 2.5.

[4] A. A. Abragam, Compt. Rend. **250**, 4334 (1960).
[5] A. A. Abragam, *L'Effet Mössbauer* (Gordon and Breach Science Publishers, Inc., New York, 1964).
[6] T. E. Cranshaw and P. Reivari, Proc. Phys. Soc. (London) **90**, 1059 (1967).
[7] J. Mishory and D. I. Bolef, *Mössbauer Effect Methodology*, edited by I. J. Gruverman (Plenum Press, Inc., New York, 1968), Vol. 4.

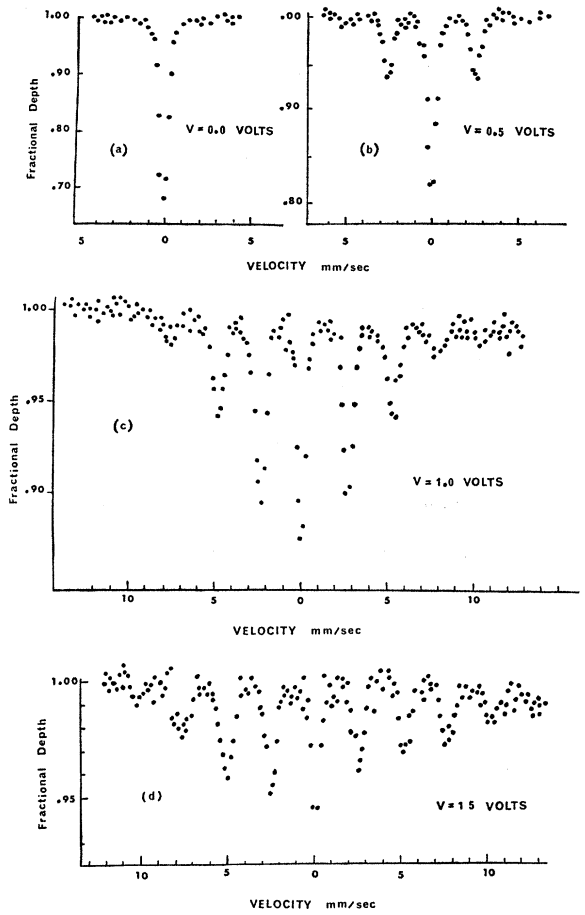

FIG. 2. Mishory and Bolef's data. Sideband spectra for a source vibrating at the ultrasonic frequency of 25 MHz; the driving voltage across the ultrasonic transducer is (a) $V=0.0$ V, (b) $V=0.5$ V, (c) $V=1.0$ V, (d) $V=1.5$ V.

with decaying amplitudes can be observed. While the analyzer is not recording, the ultrasonic vibrations are allowed to build up to their initial steady state and the procedure can be repeated.

Coincidence measurements of the 123- and 14.4-keV photons were sucessfully performed by Lynch, Holland, and Hamermesh[8] and also by Wu, Lee, Benczer-Koller, and Simms.[9] The observation of the small center-line and sideband fractions by coincidence measurements would require a prohibitively long time; the described conditions should be regarded as a thought experiment.

A. Relative Intensities of Bands Emitted from the Source

The same thought experiment can also be visualized classically.

During the lifetime of the Mössbauer nuclear excited state, the nucleus vibrates with ultrasonic frequency ω and decaying amplitude; the time-dependent projection of the amplitude in the direction of the γ beam is $a=a_0e^{-\gamma t/2}$. The retarded electric field incident on the absorber is

$$E_I{}^a(t)=\mathrm{Re}\{\exp\{i\Omega_S[t-r_0/c-(a_0/c)e^{-\gamma t/2}\times\sin(\omega t+\phi)]-\tfrac{1}{2}\Gamma_S t\}\} \quad (4)$$
$$=e^{-\Gamma_S t/2}\sum nJ_n(ka)\cos[(\Omega_S-n\omega)t-n\phi-kr_0].$$

A standard Bessel-function identity was used to prove mathematically that the damped sinusoidal motion of the source splits the electric field into infinitely many bands of frequency $\Omega_S-n\omega$; the relative weight of the bands is time-dependent.

The superscript a denotes the fact that the electric field was evaluated for one amplitude, a, only. The electric energy W_I incident on the absorber is proportional to the time integral of the square of the electric field, after proper averaging over a and ϕ was performed.

$$W_I=\sum n'\sum n''W_I{}^{n'n''}\propto\sum n'\sum n''\int_0^{2\pi}d\phi P(\phi)$$
$$\times\int_0^\infty da_0P(a_0)\int_0^\infty dtJ_{n'}(ka_0e^{-\gamma t/2})$$
$$\times J_{n''}(ka_0e^{-\gamma t/2})e^{-\Gamma_S t}\cos[(\Omega_S-n'\omega)t-n'\phi-kr_0]$$
$$\times\cos[(\Omega_S-n''\omega)-n''\phi-kr_0]. \quad (5)$$

For the diagonal terms $n'=n''$. The square of the cosine results in $\frac{1}{2}$ plus a rapidly oscillatory term. Phase angles ϕ are random; therefore, $P(\phi)=(2\pi)^{-1}$. Integration over ϕ reduces to unity for the diagonal terms.

The distribution in amplitudes, $P(a_0)$, will be discussed for two limiting cases: (a) The ultrasonic lattice vibrational mode cannot readily exchange energy with thermal vibrational modes. The result is Carruthers and Nieto's[10] Poisson distribution of eigenstates, which for large enough amplitudes implies a distribution $P(a_0)$ which is so strongly peaked that it can be approximated by a Dirac δ function. Ruby and Bolef's[3] Eq. (1) results in the limit $\gamma\to 0$. (b) The ultrasonic mode readily exchanges energy with thermal modes. Here the result is Abragam's[5] Rayleigh distribution for $P(a_0)$.

Only case (b) will be used. The integral over a_0 has a form evaluated in Ref. 11 as follows:

$$\int_0^\infty da_0a_0\langle x^2\rangle_0{}^{-1}\exp[-\tfrac{1}{2}a_0{}^2\langle x^2\rangle_0{}^{-1}]J_n{}^2(ka_0e^{-\gamma t/2})$$
$$=\exp(-k^2\langle x^2\rangle)I_n(k^2\langle x^2\rangle), \quad (6)$$

where

$$\langle x^2\rangle=\langle x^2\rangle_0e^{-\gamma t}.$$

Both a_0 and $\langle x^2\rangle_0$ are evaluated at time $t=0$. Integra-

[8] F. J. Lynch, R. E. Holland, and M. Hamermesh, Phys. Rev. **120**, 513 (1960).
[9] C. S. Wu, Y. K. Lee, N. Benczer-Koller, and P. C. Simms, Phys. Rev. Letters **5**, 432 (1960).
[10] P. Carruthers and N. M. Nieto, Am. J. Phys. **33**, 537 (1965).
[11] N. Watson, *Bessel Functions* (Cambridge University Press, New York, 1962), p. 395.

tion over a_0 expresses an average over all Mössbauer nuclei in the source. Cancellations of the exponentials $e^{-\gamma t/2}$ allowed the replacement of a by a_0 and $\langle x^2\rangle$ by $\langle x^2\rangle_0$ in most terms of the left-hand side of Eq. (6); its right-hand side reduces to Abragam's Eq. (2) in the limit $\gamma \to 0$.

For cross terms $n' \neq n''$. The square of the cosine in Eq. (5) can be expanded into terms that have $\sin\phi$ or $\cos\phi$ as multiplicative factors; integration over ϕ results in zero. Cross terms are identically zero because there is no coherent phase relationship between the Mössbauer γ emission and the ultrasonic vibrations.

Time integration of the diagonal terms can be performed after the negative exponential and hyperbolic Bessel functions are expanded into their Taylor series.

$$W_I = \sum n W_I^n \propto \tfrac{1}{2}\sum n \int_0^\infty dt f_n(t) e^{-\Gamma_S t}$$

$$= \tfrac{1}{2}\sum n \left(\sum_{l=0}^{\infty} \sum_{l'=0}^{\infty} \frac{(-y_0)^{l'} (\frac{1}{2}y_0)^{(n+2l)}}{l'!\,l!\,(n+l)!\,[\Gamma_S + (l'+n+2l)\gamma]} \right), \quad (7)$$

where

$$f_n(t) \equiv \exp(-y_0 e^{-\gamma t}) I_n(y_0 e^{-\gamma t}) \quad \text{and} \quad y_0 \equiv k^2 \langle x^2\rangle_0. \quad (8)$$

This result is exact, and the series is absolutely convergent; but for large values of y_0 it converges very slowly.

Evaluation of the double sum in l and l' for each individual value n establishes the areas under the bands. Equation (7) furnishes no information on line shapes, but their general behavior can be estimated from the plots of $f_n(t)$ against time illustrated in Fig. 3.

The behavior of $f_n(t)$ can be estimated from the large and small argument expansions of the hyperbolic Bessel functions.

$$f_n(t) \approx (2\pi y_0)^{-1/2} e^{\gamma t/2} \quad \text{provided } y \gg n^2 \text{ when } n \neq 0, \text{ and } y \gg \tfrac{1}{4} \text{ when } n = 0, \quad (9a)$$

$$f_n(t) \approx (y_0/2)^n (n!)^{-1} e^{-n\gamma t} \quad \text{provided } y \ll 1. \quad (9b)$$

In Eqs. (9), $f_n(t)$ changes exponentially with time; if Eqs. (9) are satisfied in the interval of integration before the exponential $e^{-\Gamma_S t}$ has reduced the integrand to a negligible quantity, the exponentials $e^{\gamma t/2}$ and $e^{-n\gamma t}$ establish the effective linewidths $\Gamma_S(\text{eff}) = \Gamma_S - \frac{1}{2}\gamma$ and $\Gamma_S + n\gamma$ for Eqs. (9), respectively. The line shapes are nearly Lorentzian if Eqs. (9) are good approximations.

For medium values of y there are no simple expansions but the behavior of $f_n(t)$ can be approximated to the damped sinusoidal

$$f_n(t) \approx b \sin(\beta t + \theta) e^{-\alpha t}, \quad \text{provided } y \approx n^2. \quad (10)$$

If Eq. (10) is satisfied during the main interval of integration, the widening of the top and narrowing of the wings of the line is very pronounced.

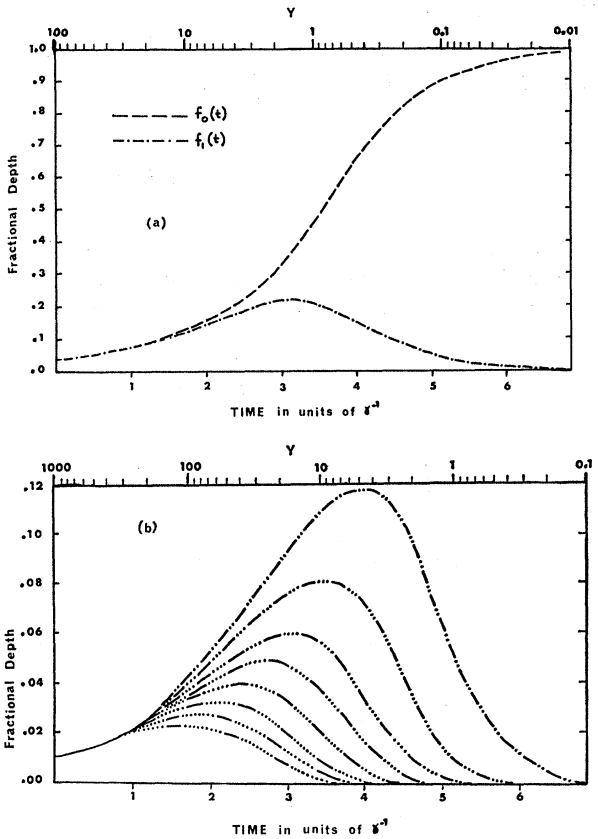

FIG. 3. Fractional depth of $f_n(t)$. The depth of center-line and sideband fractions is plotted against time on a regular and y on a logarithmic scale. (a) is $f_0(t)$ illustrated by the dashed and $f_1(t)$ by the dash-dot line; (b) shows $f_2(t)$ to $f_9(t)$. The number of dots expresses the number of the band illustrated.

B. Line Shape of Radiation Leaving Source

Exact line-shape derivations can be performed by a double Fourier transformation of the electric field prior to the integration over the Rayleigh distribution of amplitudes

$$E_I^a(t) = (2\pi)^{-1/2} \int_{-\infty}^{\infty} d\Omega e^{-i\Omega t} E_I^a(\Omega), \quad (11)$$

where $E_I^a(t) = 0$ for times $t < 0$; therefore, $E_I^a(\Omega)$ must be analytic over the bottom half of the complex plane if $\Omega > 0$.

$$\int_0^\infty dt [E_I^a(t)]^2 = \int_{-\infty}^{\infty} dt [E_I^a(t)]^2$$

$$= (2\pi)^{-1} \int\int\int_{-\infty}^{\infty} dt d\Omega d\Omega' e^{i(\Omega+\Omega')t} E_I^a(\Omega) E_I^a(\Omega'). \quad (12)$$

Time integration results in a Dirac delta function for $\Omega' = -\Omega$. The right-hand side of Eq. (12) is real, and therefore the left must be real also; this can be generally

true only if this $E_I{}^a(\Omega)=E_I{}^{a*}(-\Omega')$.

$$W_I \propto \int_0^{2\pi} d\phi\, P(\phi) \int_0^{\infty} da_0 P(a_0) \int_{-\infty}^{\infty} d\Omega |E_I{}^a(\Omega)|^2 \equiv \int_{-\infty}^{\infty} d\Omega |E_I(\Omega)|^2. \quad (13)$$

The last step in Eq. (13) is the definition of $E_I(\Omega)$. Integrations over a_0 and ϕ can be performed after $E_I{}^a(\Omega)$ is evaluated by an inverse Fourier transformation.

$$W_I=\sum n \int_{-\infty}^{\infty} d\Omega W_I{}^n(\Omega) \propto (2\pi)^{-1} \int_0^{\infty} da_0 P(a_0) \times \int\int_{-\infty}^{\infty} d\Omega dt' dt'' e^{i\Omega(t'-t'')} E_I{}^a(t') E_I{}^a(t'')$$

$$=\sum n (2\pi)^{-1} \int_{-\infty}^{\infty} d\Omega \int\int_0^{\infty} dt' dt'' f_n(t',t'') \times \exp[i\Omega_I{}^n(t'-t'')-\tfrac{1}{2}\Gamma_S(t'+t'')], \quad (14)$$

where

$$f_n(t',t'') \equiv \exp[-\tfrac{1}{2}y_0(e^{-\gamma t'}+e^{-\gamma t''})] \times I_n(y_0 e^{-\gamma(t'+t'')/2}) \quad (15)$$

and

$$\Omega_I{}^n \equiv \Omega-(\Omega_S-n\omega).$$

Integration over ϕ reduces to unity. Integration over a_0 is still possible by an amendment of Eq. (6). The lower limit of the time integration was changed to zero, because $E_I{}^a(t)=0$ when $t<0$. The double time integration can be performed after $f_n(t',t'')$ is expanded into a triple infinite series and the changes of variables $T=t'+t''$ and $t=t'-t''$ performed. The result is

$$W_I{}^n(\Omega) \propto \sum \frac{c_{n,y,l,l',l''}}{\Gamma_S+(l'+l''+n+2l)\gamma} \times \left\{ \frac{\Gamma_S+(2l'+n+2l)\gamma}{[\tfrac{1}{2}\Gamma_S+(l'+\tfrac{1}{2}n+l)\gamma]^2+(\Omega_I{}^n)^2} \right\}, \quad (16)$$

where

$$\sum c_{n,y,l,l',l''} \equiv \sum_{l=0}^{\infty} \sum_{l'=0}^{\infty} \sum_{l''=0}^{\infty} (-1)^{(l'+l'')} \frac{(\frac{1}{2}y_0)^{(l'+l''+n+2l)}}{l'!l''!l!(n+l)!}. \quad (17)$$

Equation (16) was solved on the General Electric time sharing service computer by the reduction of a three-dimensional matrix to a series in $r=l+l'$.

$$W_I{}^n(\Omega) \propto \sum r\, g_{n,y,r}[\Gamma_S+(2r+n)\gamma] \{\tfrac{1}{4}[\Gamma_S+(2r+n)\gamma]^2+(\Omega_I{}^n)^2\}^{-1}. \quad (16')$$

Each factor $g_{n,y,r}$ is an alternating series in y_0; the resultants have alternating signs. Equation (16′) expresses a superposition of Lorentzian lines of increasing width. If $y_0<1$ the first term ($r=0$) is the dominant one; a wider line with less area has to be subtracted; the result is line narrowing mainly at the wings; this narrowing combined with a departure from the Lorentzian shape becomes more pronounced with increasing y_0, until the character of the line approaches the Gaussian.

For values of $y_0>1$, the first term in Eq. (16′) is not numerically largest; line narrowing beyond the natural width Γ_S is also possible for the sidebands if y_0 is substantially larger than n^2.

This information can be read from the plots of $f_n(t)$ against time in Fig. 3. The maxima occur at a value of y that is of the same order but slightly larger than n^2. In case $f_n(t)$ increases during the main interval of integration the line is narrowed beyond the natural width.

C. Effect of Absorber

Each monochromatic component of the electric field is capable of exciting resonant electric vibrations in the absorber if the Doppler-modulated natural frequency of the absorber, Ω_A, is approximately equal to the incident frequency Ω; small changes in the relative velocity between the source and absorber successively bring the sidebands into resonance.

A good explanation of resonant absorption with the help of the imaginary part of the dielectric constant ϵ is given, for instance, by Stratton[12]:

$$\epsilon \approx \epsilon_0\{1+b[(\Omega^2-\Omega_A{}^2)\pm i\Omega\Gamma_A]^{-1}\} \approx \epsilon_0\{1+b[2\Omega(\Omega-\Omega_A\pm\tfrac{1}{2}i\Gamma_A)]^{-1}\}. \quad (18)$$

Here b is a parameter proportional to the number of atoms per unit volume capable of resonant absorption and the fraction of the incoming γ beam that they can absorb resonantly. For the ultrasonically vibrating source, this fraction is the Mössbauer fraction f_A for the temperature of the absorber; for the ultrasonically vibrating absorber, f_A has to be replaced by $f_n(t)$; therefore, the factor b becomes time-dependent also.

By straightforward application of Maxwell's equations, it is possible to show that the complex dielectric constant introduces an imaginary part to the wave propagation vector k; in the vacuum k is purely real and has the magnitude $\Omega(\mu_0\epsilon_0)^{1/2}=\Omega/c$, but in the medium,

$$k=(\Omega^2\mu\epsilon\pm i\sigma\mu\Omega)^{1/2} \approx \Omega/c + b(\Omega-\Omega_A\mp\tfrac{1}{2}i\Gamma_A)\{4c[(\Omega-\Omega_A)^2+\tfrac{1}{4}\Gamma_A{}^2]\}^{-1}. \quad (19)$$

The sign ambiguity is present because Eq. (19) applies both to resonant absorption and stimulated emission; a negative real part of ikx describes absorption.

The factor b can be identified in terms of Margulis and Ehrman's[13] normalized absorber thickness T_A, which

[12] J. A. Stratton, *Electromagnetic Theory* (McGraw-Hill Book Co., New York, 1941), p. 321.

[13] S. Margulis and J. R. Ehrman, Nucl. Instr. Methods **12**, 131 (1961).

should not exceed 20.

$$T_A \equiv bD/\Gamma_A c \equiv Bf_A. \tag{20}$$

Mössbauer frequencies are of the order of 10^{20} sec^{-1}; at such high frequencies $b \ll \Omega_A \Gamma_A$ if $T_A < 20$; at high frequencies, $\mu \to 1$ and $\sigma \to 0$. Equation (18) was inserted into Eq. (19), and only the two leading terms in the binominal expansion were carried. After passage through an absorber of thickness D, each monochromatic component of the electric energy is reduced to

$$|E_T(\Omega)|^2 = |e^{ikD}E_I(\Omega)|^2 = \exp(-b\Gamma_A D\{4c[(\Omega-\Omega_A)^2+\tfrac{1}{4}\Gamma_A{}^2]\}^{-1}) \times |E_I(\Omega)|^2. \tag{21}$$

The observable is the reduction in transmitted energy caused by resonant absorption. In the absence of resonance, the absorber is nearly transparent to Mössbauer radiation. Absorption processes other than Mössbauer are insensitive to small changes in relative velocity; therefore, their contribution can be expressed by a multiplicative constant.

To simplify notation, contributions of neighboring bands will be omitted; they can easily be added later. The observable is

$$W_I{}^n(\Omega_A) - W_T{}^n(\Omega_A) \propto (2\pi)^{-1}\int_{-\infty}^{\infty} d\Omega |E_I{}^n(\Omega)|^2 \times (1-\exp\{-Bf_A\Gamma_A[4(\Omega-\Omega_A)^2+\Gamma_A{}^2]^{-1}\}), \approx \tfrac{1}{4}\Gamma_A B f_A \sum r\, g_{n,y,r}[\Gamma+(2r+n)\gamma] \times \{\tfrac{1}{4}[\Gamma+(2r+n)\gamma]^2+(\Omega_T{}^n)^2\}^{-1}, \tag{22}$$

where

$$\Gamma \equiv \Gamma_S+\Gamma_A,\ \Omega_T{}^n \equiv \Omega_A-(\Omega_S-n\omega). \tag{23}$$

Equation (22) was derived by an expansion of the resonant exponential into its Taylor series carrying only the term linear in Bf_A; this is the thin absorber approximation. Contour integration can be performed around a pole of order unity, if the electric energy is Fourier transformed into the double-time integral equation (14).

4. QUANTITATIVE EVALUATION

A. Comparison of Incident and Transmitted Line Shapes

At first sight it seems that Eqs. (22) and (16′) are equivalent except for the replacement of Γ_S by Γ and a multiplicative constant; this would indicate that the passage through the absorber only increases the linewidth by Γ_A without changing the shape. In reality the weight of the different terms in the series expansion in r is changed because in both equations $g_{n,y,r}$ has a function of Γ_S not Γ in the denominator.

Examination of the plots of $f_n(t)$ shows that for values of $y_0 > n^2$ it is possible that the main interval of integration has to be extended far enough beyond the maximum of $f_n(t)$ to cause line widening of the radiation leaving the source. In the evaluation of the line shape of the transmitted energy the damping factor is increased from Γ_S to $\Gamma_S+\Gamma_A$; the integrand might be very small when the maximum of $f_n(t)$ is reached. The result is a line with width at half-height that is greater than Γ_S for the incident, but smaller than Γ for the transmitted, radiation.

Table I shows the comparison of the incident and transmitted line shapes for $n=1$, $\gamma=\Gamma_S$, and various

TABLE I. Data for the first sideband at various values of y_0. Different linewidths evaluated for each datum show the departure from the Lorentzian shape. Γ_S(rel)$=\Gamma_S$(eff)$/\Gamma_S$; Γ(rel)$=\Gamma$(eff)$/\Gamma$. In the lower half of the table the observable line depth is expressed in units of $\frac{1}{4}Bf_1(t=0)$.

	$y_0=0.5$		$y_0=1.0$		$y_0=1.5$		$y_0=2.0$		$y_0=2.5$	
$\Omega_I{}^1$	depth	Γ_S(rel)	depth	Γ_S(rel)	depth	Γ_S(rel)	depth	Γ_S(rel)	depth	Γ_S(rel)
0.00	0.2481		0.2872		0.2584		0.2142		0.1724	
0.20	0.2432	1.38	0.2807	1.32	0.2519	1.26	0.2084	1.19	0.1674	1.16
0.40	0.2293	1.38	0.2627	1.31	0.2341	1.25	0.1923	1.18	0.1535	1.14
0.60	0.2092	1.38	0.2368	1.30	0.2084	1.23	0.1693	1.16	0.1338	1.12
0.80	0.1860	1.38	0.2071	1.28	0.1794	1.20	0.1434	1.13	0.1118	1.08
1.00	0.1623	1.37	0.1772	1.26	0.1505	1.18	0.1180	1.10	0.0903	1.05
1.20	0.1400	1.37	0.1495	1.24	0.1241	1.16	0.0951	1.07	0.0712	1.01
1.40	0.1201	1.36	0.1252	1.22	0.1013	1.13	0.0757	1.04	0.0553	0.96
1.60	0.1028	1.35	0.1046	1.21	0.0824	1.11	0.0599	1.00	0.0425	0.91
1.80	0.0881	1.34	0.0875	1.19	0.0670	1.07	0.0473	0.96	0.0325	0.87
2.00	0.0758	1.33	0.0734	1.17	0.0547	1.04	0.0374	0.92	0.0249	0.82
$\Omega_T{}^1$	depth	Γ(rel)	depth	Γ(rel)	depth	Γ(rel)	depth	Γ(rel)	depth	Γ(rel)
0.00	0.1427		0.1585		0.1373		0.1100		0.0860	
0.20	0.1386	1.17	0.1535	1.13	0.1325	1.05	0.1058	1.00	0.0825	0.98
0.40	0.1277	1.17	0.1400	1.11	0.1197	1.04	0.0948	0.99	0.0733	0.97
0.60	0.1128	1.16	0.1218	1.09	0.1026	1.03	0.0801	0.98	0.0612	0.95
0.80	0.0967	1.16	0.1025	1.08	0.0848	1.02	0.0651	0.96	0.0490	0.93
1.00	0.0815	1.15	0.0847	1.07	0.0687	1.00	0.0517	0.94	0.0382	0.90
1.20	0.0682	1.15	0.0695	1.06	0.0552	0.98	0.0407	0.92	0.0296	0.87
1.40	0.0570	1.15	0.0570	1.05	0.0444	0.97	0.0322	0.90	0.0230	0.85
1.60	0.0479	1.14	0.0470	1.04	0.0360	0.95	0.0256	0.88	0.0180	0.83
1.80	0.0405	1.14	0.0391	1.03	0.0294	0.94	0.0207	0.87	0.0144	0.81
2.00	0.0345	1.13	0.0328	1.02	0.0244	0.93	0.0169	0.85	0.0116	0.80

values of y_0 in the vicinity of n^2. For each value of y_0, the left-hand column contains machine-calculated data, and the right-hand column contains an evaluation of the departure from the Lorentzian shape. For each individual datum the width of a Lorentzian line to which it would belong was derived; it is the ratio of this effective width to Γ_S or Γ that is tabulated. This unusual description of the line shape shows the widening of tops and narrowing of wings of lines more clearly than standard methods.

For the transmitted radiation the linewidth at half-height is Γ when $y_0=1.5$ and smaller than Γ for $y_0=2$, 2.5. The incident radiation has linewidths at half-height that exceed Γ_S for all tabulated cases, but narrowing of the wings is very dominant for the larger values of y_0.

B. Optimum Line Narrowing of Center Line

At first sight it seems possible that γ can approach $2\Gamma_S$; the linewidth of the radiation leaving the source seems to approach zero.

This result is fallacious because it was derived using only the leading term in the large argument expansion of the hyperbolic Bessel function, Eq. (9a). The approximation is only valid provided the inequality $y \gg \frac{1}{4}$ is reasonably well satisfied in the entire interval of integration; this is impossible when γ approaches $2\Gamma_S$ because the integrand remains nearly constant until y approaches n^2.

Cranshaw and Reivari used y of the order of 50 in their steady-state experiment and were able to observe center-line fractions of slightly over 1% at these high ultrasonic amplitudes. It is therefore realistic to assume y_0 of the order of 50 and choose $\gamma=1.2\Gamma_S$; only first-order corrections that widen the top of the line are necessary. A linewidth of $0.4\Gamma_S$ with a line depth of the order of 1% is in the realm of possibility for the radiation leaving the source.

It would be fallacious to simply double the damping factor and reach the optimistic conclusion that the observable can be 0.4Γ. The derivation of the effect of the absorber on the radiation leaving the source, established in the previous paragraph, would result in the pessimistic value of 0.7Γ for the observable.

More careful considerations of the optimum conditions for the line shape of the radiation that passed through the absorber results in a possible linewidth of about 0.55Γ without excessive widening of the top of the line.

5. DISCUSSION OF EXPERIMENTAL DATA

In this section the data from Cranshaw and Reivari's[7] and Mishory and Bolef's[8] experiments will be compared. A very interesting feature in Cranshaw and Reivari's data is the sag in the background combined with near sidebands that are not wider than the center line.

A. Mishory and Bolef's Data

The width of the center line slightly decreases with increasing ultrasonic amplitude; sidebands are progressively widened with increasing n; this progressive widening is more pronounced for the higher than lower amplitudes of ultrasonic vibrations.

Mishory and Bolef reported a line depth of the center line which is slightly above their expected value for high-amplitude ultrasonic vibrations; they explained it by a reduction of the self-absorption of the source in the presence of ultrasonic vibrations. Self-absorption also widens the Mössbauer line; therefore, the line narrowing of the center line is explainable by a reduction in self-absorption.

A possible explanation of the widening of the sidebands is a statistical distribution over a range $\Delta\omega$ of ultrasonic frequencies. The contribution of one Mössbauer event to the nth sideband is at a distance $n(\omega\pm\Delta\omega)$ from the center line. This widens the nth sideband to $\Gamma+2n\Delta\omega$. Mishory and Bolef's data would indicate that $\Delta\omega$ is larger for high-amplitude ultrasonic vibrations, which is an expected result.

Mishory and Bolef did not investigate the linewidth of sidebands in detail; other explanations, besides the one given in the previous paragraph, might be possible.

B. Cranshaw and Reivari's Data

In the absence of ultrasonic vibrations, Cranshaw and Reivari's center linewidth is approximately 3Γ, but in the presence of their high amplitude vibrations it is narrower. The near sidebands are not wider than the center line.

In the presence of high-amplitude ultrasonic vibrations Margulis and Ehrman's[13] effective absorber thickness is drastically reduced; a reduction in line widening results which exceeds the narrowing effect of Mishory and Bolef's reduction of self-absorption in the vibrating source. Reduction in effective absorber thickness can explain narrow center lines, but not the fact that center line and sidebands have the same width. Cranshaw and Reivari's ultrasonic frequency of 16 MHz is lower than Mishory and Bolef's 25 MHz; this would indicate a reduction in $\Delta\omega$. Cranshaw and Reivari's amplitudes are several times as large as Mishory and Bolef's; this would probably over compensate the reduction in $\Delta\omega$ caused by the lower frequency.

Cranshaw and Reivari's Mössbauer nuclei are evenly distributed in a layer of Perspex cement; interference phenomena can cause increases or decreases of ultrasonic vibrational amplitudes during the average Mössbauer nuclear excited-state lifetimes. These changes in amplitudes are as likely to cause line narrowing as widening. The sag in Cranshaw and Reivari's background is too deep to be only caused by the contribution of tails of neighboring lines, but might be instrumental. An interesting explanation might be a sag that is caused

by widened lines that grew together; superimposed would be the narrowed lines.

An increase in ultrasonic amplitudes during the average Mössbauer nuclear excited-state lifetime can cause considerable line narrowing if $y_0 < n^2$. This narrowing mechanism increases in likelihood with increasing n, and possibly balances the widening caused by the statistical distribution in ultrasonic frequencies present.

Such increases or decreases in ultrasonic amplitudes of the individual Mössbauer nuclei are much less likely in Mishory and Bolef's source, where the Co^{57} nuclei are in a very thin top layer that obeys boundary conditions.

C. Possible Experimental Verifications of Line Narrowing

The superposition of narrowed and widened lines can be experimentally verified by controlled amplitude modulation of the ultrasonic vibrations. The choice of the envelope of the vibrational amplitudes is at the experimentalist's disposal. The exact shape of the center line and sidebands can then be analyzed.

A periodic 180° phase change in the driving voltage of the ultrasonic transducer also causes damping and subsequent build-up of vibrational amplitudes; comparison of the two effects could give an indication of damping mechanisms of ultrasonic vibrations in solids.

At first sight it seems possible to record only the time periods in which $f_n(t)$ increases, discarding the widened lines. This would require time intervals in which the multichannel analyzer is not recording. The Mössbauer events would be evenly distributed over periods of recording that terminate with the maximal $f_n(t)$. A discrimination against long-lived events at the end of the interval of recording would take place that would counteract the line narrowing. Machine calculations for such intervals of recording were performed; the interesting result is an optimum condition of natural linewidth.

A net narrowing effect might not be observable in a realistic experiment. The reason why narrowing could still be demonstrated is that the superposition of a widened and a narrowed Lorentzian line can not be a Lorentzian of natural width.

6. CONCLUSIONS

The effect of ultrasonic vibrations with decaying amplitudes has been analyzed. The main distinction between the derivations of this paper and the ones performed by Nussbaum and Dash[1] for a Mössbauer source that did not reach thermal equilibrium is the fact that not only the center line but also sidebands can be analyzed. Of great importance is the slow approach of the center-line fraction to zero when the ultrasonic vibrational amplitude increases. Cranshaw and Reivari were able to observe a center-line fraction of over 1% in the presence of ultrasonic vibrational amplitudes of the order of 1Å. For such root-mean-square displacements of thermal vibrations the Mössbauer fraction would be an infinitesimal. The reason is the coherence of the ultrasonic vibrations; the higher-order terms in the series expansion of the hyperbolic Bessel functions have the same width as the leading term; this is not the case for localized lattice vibrational modes.

An optimum condition for line narrowing caused by ultrasonic vibrations with decaying amplitudes can be estimated from the length of the time interval in which the large argument asymptotic expansion Eq. (9a) is valid. During this interval, the ultrasonic vibrational amplitude is reduced by several orders of magnitude. It is not surprising that a considerably higher percentage of line narrowing can be achieved than for a localized lattice vibration mode with decaying amplitude in the cooling source.

The center line is always narrowed in the presence of ultrasonic vibrations with decaying amplitudes; the sidebands may be narrowed or widened, depending on the initial amplitudes. It is not legitimate to assume that the effect of a thin absorber is a simple increase of the linewidth by Γ_A without changing the line shape. Examples are given where the linewidth of the radiation leaving the source exceeds Γ_S but the width of the observable line analyzed by the absorber is less than $\Gamma_S+\Gamma_A$. Such lines have much wider tops but narrower wings than the typical Lorentzian shape.

Changes in ultrasonic vibrational amplitudes might be responsible for the lack of line widening of Cranshaw and Reivari's sidebands. This interesting phenomenon could be investigated with the use of controlled variations in amplitudes.

The derivations performed in this paper might be of value for the verification of the interesting phenomenon of line narrowing of the Mössbauer line beyond its natural width. These derivations are much simpler than those performed by Harris; yet they are conceptually similar enough to be regarded as an ultrasonic analog to the cooling source. The thought experiment on which the calculations are based might be as difficult to verify as the decaying localized lattice vibrational mode in the cooling source, but the superposition of narrowed and widened lines which do not add up to lines of natural width have a good chance of experimental verification.

ACKNOWLEDGMENTS

I am very grateful to Dr. W. M. Visscher, whose valuable advice helped me throughout this work, and to Dr. S. Ruby and Dr. D. I. Bolef for the fruitful discussions on ultrasonics. My sincerest thanks go also to Dr. Roark and J. Randack who independently helped me with two different computer programs.